THE ASTROPHYSICAL JOURNAL, 487:L181–L185, 1997 October 1
© 1997. The American Astronomical Society. All rights reserved. Printed in U.S.A.

PULSED OPTICAL EMISSION FROM PSR 0656+14[1]

A. SHEARER
Information Technology Centre, University College Galway, Galway, Ireland
R. M. REDFERN, G. GORMAN, R. BUTLER, A. GOLDEN, AND P. O'KANE
Department of Physics, University College Galway, Galway, Ireland
G. M. BESKIN, S. I. NEIZVESTNY, V. V. NEUSTROEV, AND V. L. PLOKHOTNICHENKO
Special Astrophysical Observatory, Nizhnij Arkhyz, Karachai-Cherkessia, Russia
AND
M. CULLUM
European Southern Observatory, Garching, München, Germany
Received 1997 April 23; accepted 1997 July 21; published 1997 September 2

ABSTRACT

Using data collected with the Special Astrophysical Observatory (SAO) 6 m telescope and the University College Galway (UCG) Transputer Instrument for Fast Image Deconvolution (TRIFFID) imaging photometer, we show that the radio, X-ray, and γ-ray pulsar PSR 0656+14 exhibits pulsed optical emission. We observed that the pulsed fraction was consistent with 100% and that the flux was higher than that expected from a thermal source. The magnitude of PSR 0656+14 in the *B* band was observed to be 25.1 ± 0.3, consistent with previous CCD observations. The peak of the optical signal is at phase 0.2 compared to the radio and in phase with the weak γ-ray pulse.

Subject headings: instrumentation: detectors — pulsars: individual (PSR 0656+14)

1. INTRODUCTION

Only three pulsars have been seen to emit pulsed optical radiation, namely, PSR 0532+21 in the Crab Nebula (first observed as an optical pulsar in 1968; Cocke, Disney, & Taylor 1969), PSR 0833−45 (the Vela pulsar; Wallace et al. 1977), and PSR 0540−69 in the LMC (Middleditch & Pennypacker 1985). Subsequently, integrated optical signals have been found for three pulsars (Geminga, PSR 0656+14, and PSR 1509−58; see Bignami & Caraveo 1996; Caraveo, Bignami, & Mereghetti 1994a; Caraveo, Mereghetti, & Bignami 1994b) at magnitudes greater than would be expected by scaling from the Crab pulsar (Pacini & Salvati 1987), and thermal unpulsed emission has been detected from PSR 0950+08 and PSR 1929+10 (Pavlov, Stringfellow, & Córdova 1996). More recently PSR 1055−52 has been observed with the *Hubble Space Telescope* (*HST*) (Mignani, Caraveo, & Bignami 1997). Most recently, an optical millisecond pulsar has been proposed in the remnant of SN 1987A (Middleditch et al. 1996). These pulsars make a diverse group, whose optical emission is not adequately explained by theory.

Historically, most of our information about pulsars has come from studies of their radio emission. However, with the advent of sensitive satellite-borne X-ray and γ-ray detectors, there is now being established a statistically significant sample of higher energy emitters. While for most young pulsars the emission is dominated by nonthermal radiation (presumed to be magnetospheric in origin), for middle-aged pulsars [$\tau \approx (0.1\text{–}10) \times 10^5$ yr] thermal radiation from the cooling neutron star surface or atmosphere can dominate, particularly in the EUV and soft X-ray bands. In the optical region we have the intriguing position that the thermal and nonthermal radiation are roughly comparable, which makes it a particularly useful wave band for studying emission mechanisms for pulsars of all ages. Previous optical studies have been hampered by the extreme faintness of the objects, which has precluded detections of their integrated fluxes, let alone pulsed emission. However, by using two-dimensional photon counting imaging detectors, the effective photometer sky aperture can be reduced, compared with conventional photometers. This is because much of the required astrometric analysis can be performed off-line, to greater precision than can be achieved in real time, and because effects such as telescope wobble that necessitate a large aperture can be entirely removed (Shearer et al. 1994). Photons chosen for analysis can be selected in software from an aperture matched (to maximize signal-to-noise ratio) to the prevailing seeing and background conditions, and their arrival times can be subjected to time series analysis. Very large (>25) signal-to-noise ratio improvements can be achieved compared to conventional single-pixel aperture photometry.

PSR 0656+14 was first observed as a radio pulsar in the second Molongo pulsar survey (Manchester et al. 1978). From these and other radio observations, the pulsar was seen to have a characteristic age ($\tau = 2P/\dot{P}$) of 1.1×10^5 yr and a surface magnetic field of 4.7×10^{12} G (Taylor et al. 1993). The object is almost in the center of a large circular X-ray emitting ring (the Gemini-Monoceros enhancement); however, radio observations (Thompson & Córdova 1994) indicate that it has a proper motion that is taking it toward the center of the ring, which casts doubt on this feature being the remains of the pulsar's associated supernova remnant. High-energy observations have shown that the pulsar is a source of ultrasoft X-rays and a weak source of high-energy γ-rays (Córdova et al. 1989; Thompson et al. 1991; Ramanamurthy et al. 1996). *Extreme Ultraviolet Explorer* (*EUVE*) observations (Foster, Edelstein, & Bowyer 1996) showed no evidence of pulsations consistent with the weakly modulated soft X-ray flux and with the *EUVE* emission coming from the whole neutron star surface rather than a restricted region such as a hot polar cap. The optical counterpart to PSR 0656+14 has been proposed as a faint star ($m_v \approx 25$), roughly coincident with the radio position (Caraveo et al. 1994a). The optical observations of Mignani et al. (1997)

[1] Based on observations taken at the Special Astrophysical Observatory of the Russian Academy of Sciences at Nizhnij Arkhyz, Russia.

TABLE 1
OBSERVATION LOG

Date	Exposure (s)	Filter	Seeing (arcsec)
1996 Jan 14, 20:22:31	102	*B*	1.8
1996 Jan 14, 20:26:26	1180	*B*	1.9
1996 Jan 14, 20:46:57	5228	*B*	1.6
1996 Jan 15, 19:04:43	2215	*B*	1.4
1996 Jan 15, 20:37:03	5748	*B*	1.5

and Kurt et al. (1996) give magnitudes of ≈25 *V* and 24.85 *B*, respectively. The Kurt et al. (1996) results are particularly important to this work, as they were taken with the same telescope at a similar time. Although this is brighter than expected from a pure synchrotron or a pure thermal origin of the optical radiation, *HST* observations (Pavlov et al. 1996; Mignani et al. 1997) have increased the likelihood that the proposed star is indeed the optical counterpart. The brightness of the candidate can be explained by a combination of nonthermal radiation and thermal emission enhanced by atmospheric effects (Pavlov et al. 1996). Using conventional photometers, only very poor upper limits are achievable for determining pulsed emission. This work describes observations taken with a two-dimensional photon counting system with high time resolution.

2. OBSERVATIONS

Observations were made over three nights in 1996 January, using the 6 m telescope of the Special Astrophysical Observatory (SAO), and a two-dimensional photon counting Multiple Anode Microchannel-Plate Array (MAMA) detector with a bialkali photocathode (Cullum 1990; Timothy & Bybee 1986). This type of detector uses a microchannel plate and an array of anodes to give the precise location and time of arrival of incident photons. The time tagging and data recording system of the University College Galway (UCG) Transputer Instrument for Fast Image Deconvolution (TRIFFID) camera (Redfern et al. 1993) was used to record the arrival time and two-dimensional position of each photon to a precision of 1 μs and 25 μm, corresponding to an equivalent spatial resolution of 0.″22 on the 6 m telescope. Timing was achieved using a combination of a Global Positioning System receiver, which gave UTC to a precision of 400 ns every 10 s, and an ovened 10 MHz crystal. Over the duration of the observations the ovened crystal was found to be constant to less than 1 μs per 10 s interval. On each night the Crab pulsar was observed for calibration purposes. Table 1 shows a log of the PSR 0656+14 observations used in the final analysis.

3. DATA REDUCTION

The photon positions were binned to produce an image after each exposure. By using the normal TRIFFID image processing software, the images were marginally improved by removing the effects of telescope movement (Shearer et al. 1996a). These separate images were then summed to produce one deep image. Figure 1 shows an intensity contour plot of the region around the pulsar. The summed image was compared with New Technology Telescope (NTT) images taken of the same region (Caraveo et al. 1994a). Using the IRAF GEOMAP, GEOTRAN, and GEOXYTRAN routines, the position of the candidate was determined on each of our images. The average residual in the transformation was better than 0.1 (0.″022) MAMA pixels in the region of PSR 0656+14. The photon arrival times were

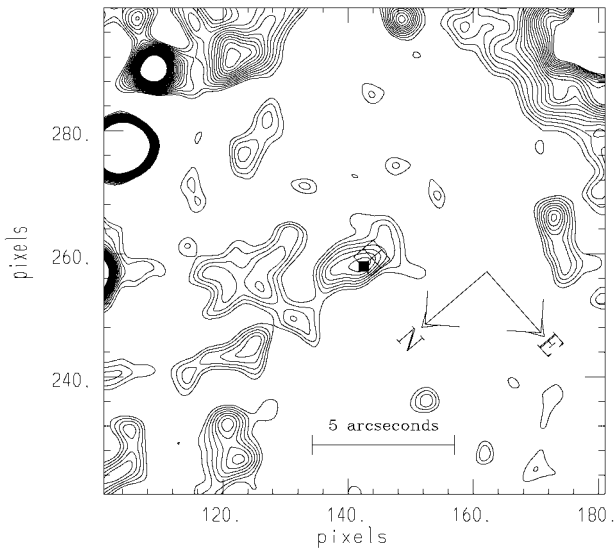

FIG. 1.—A contour plot of the intensities seen around PSR 0656+14. The data are a section of the sum of our five images. Ten contours are evenly spaced above background. The cross marks the position of the radio pulsar, and the filled square indicates the position of the center of the photometer aperture.

extracted from a window with a diameter corresponding to 0.″7. The window size was chosen to maximize our signal-to-noise ratio given our observed point-spread function and count rate. Only those data that had a final image FWHM of less than 2.″0, taken under photometric conditions, were selected for final analysis. This excluded one night in which the seeing was always worse than 2.″2.

The extracted times were then translated to the solar system barycenter using the JPL DE200 ephemeris. Combining the Crab pulsar observations over four nights indicated a night-night absolute timing accuracy of better than 10 μs. The Lyne and Pritchard Crab pulsar timing ephemeris (Lyne & Pritchard 1996) was used to determine the peak of the Crab pulse; phase was maintained to within 10 μs over the whole period. The data from PSR 0656+14 were then folded in phase with the radio timing ephemeris (Arzoumanian, Nice, & Taylor 1992; Arzoumanian et al. 1994; Camilo 1996): our ephemeris was $f = 2.5981590577062\ \mathrm{s}^{-1}$; $\dot{f} = -3.71338 \times 10^{-13}\ \mathrm{s}^{-2}$, referenced to Julian Date 2,449,029.505166924. The data were then analyzed with a 2×10^6 point fast Fourier transform (FFT) with a bin width of 44.37 ms. A total of 18,708 counts were observed in the 0.″7 aperture during the 14,473 s of observation. The number of background counts was 18,150, determined using the IRAF DAOPHOT package as described below. Figure 2 shows the power spectrum from the FFT analysis. The peak signal from this figure was at the exact pulsar spin-down period for these observations.

Figure 3 shows the *B* light curve folded with the radio ephemeris. In this figure ≈1815 photons bin^{-1} come from sky background. The peak optical signal is at phase 0.2, in close agreement with the γ-ray data (Ramanamurthy et al. 1996). The significance of such a phase plot is best given by the phase-independent Rayleigh statistic (Buccheri et al. 1983), which gives a probability for a chance occurrence of 0.19% for this data set. The significance of the power spectrum signal is more difficult to determine. A 7.4 σ peak is observed at the exact spun-down radio frequency, corresponding to a probability of $\approx 6 \times 10^{-4}$ in an FFT analysis. This gives a better estimate of

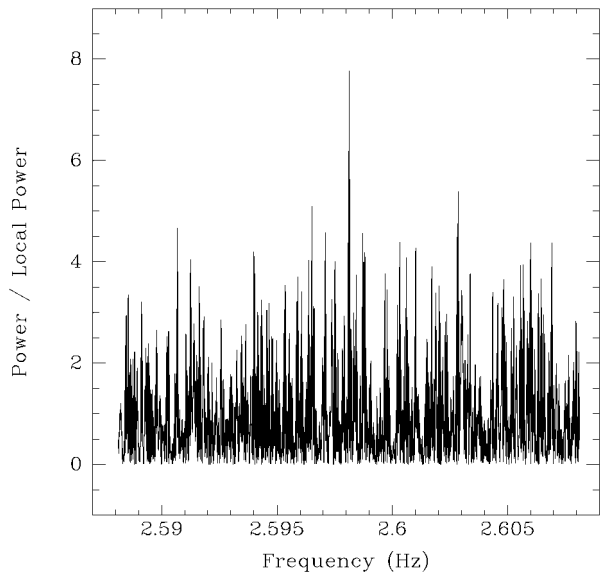

FIG. 2.—The FFT power spectrum of the region around the spun-down radio frequency. The peak is within 10 μHz of the radio frequency.

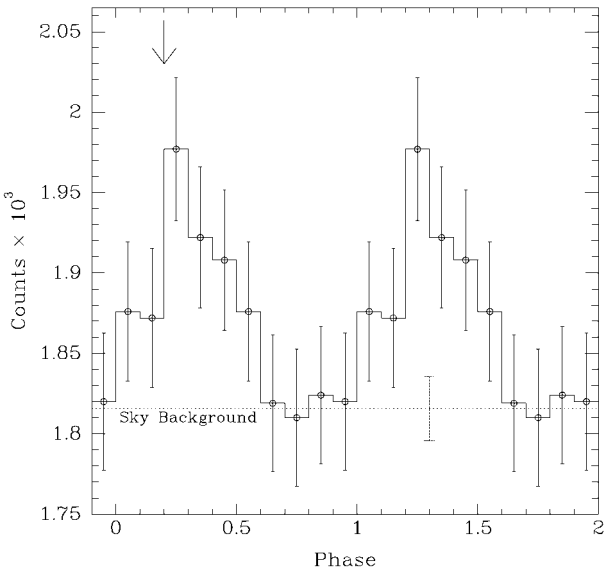

FIG. 3.—The phase plot of the optical light curve from PSR 0656+14. Two phases are shown for clarity, with Poissonian error bars for each point. Our data are folded using the radio ephemeris with the radio pulse occurring at phase 0, and the γ-ray peak is marked with an arrow. The mean sky background and error in the vicinity of the pulsar are marked with dotted lines.

the significance, as an FFT power spectrum is the most sensitive test for sinusoidal signals. The derived peak frequency was independent of any other ephemeris. Stars 31 and 32 of Halpern & Tytler (1988), in the field around the Geminga pulsar, were observed on the first night of these observations and were used for a magnitude calibration. Comparisons with the Crab pulsar and stars in the PG 0220 field (Landolt 1992) showed a degree of nonlinearity (Shearer et al. 1996a) that led to an initial underestimate of the brightness of the pulsar. Comparisons with other stars in the PSR 0656+14 field coincident on our images and with a CCD image taken with the ESO NTT ESO Multi-Mode Instrument (EMMI) camera indicated that the TRIFFID system for these observations was linear for stars fainter than 18th magnitude in *B*. To determine the pulsed fraction, the background level around the pulsar was measured from our integrated images using the IRAF RADPROF and PHOT routines to produce an average radial profile around the pulsar. This background level is shown in Figure 3. Our signal is consistent with a pulsed fraction between 40% and 100% (using a conservative 3 σ unpulsed limit); however, it must be stressed that this is highly dependent upon the errors in determining the background level. From the integrated images we get a total *B* magnitude of 25.1 $\pm$ 0.3; the main uncertainty comes from determining the background level. This figure corrects that reported in Shearer et al. (1996b). This corresponds to a flux of 3.9×10^{-30} ergs cm^{-2} s^{-1} Hz^{-1}, with a 1 σ upper limit on the unpulsed flux of 8×10^{-31} ergs cm^{-2} s^{-1} Hz^{-1}. Our analysis should yield similar results for different sky pupils, albeit with lower significance.

4. DISCUSSION

Previous estimates (Caraveo et al. 1994a) indicated an approximate integrated *V* magnitude of 25, corresponding to a flux of 3.5×10^{-30} ergs cm^{-2} s^{-1} Hz^{-1} (Caraveo et al. 1994a; Mignani et al. 1997). The distance to PSR 0656+14 is very uncertain, varying from 760 pc from radio dispersion measures (Taylor et al. 1993), to an estimate of 200–500 pc from X-ray observations. Adopting a distance of 288 pc (Pavlov et al. 1996) and assuming 1 sr beaming angle, we obtain for our *B* flux a pulsed *B*-band luminosity $\approx 4 \times 10^{26}$ ergs s^{-1}. Given our pulse shape, with a roughly 30% duty cycle, we can infer that the real beam size is in the region 3–4 sr, depending upon whether a pencil or fan beam was produced. In this case we have a *B* luminosity of ≈ 1–2×10^{27} ergs s^{-1}. Reddening at this distance and location is unlikely to be significant in suppressing the *B* magnitude (Pavlov et al. 1996). The efficiency of producing these optical photons from the spin-down energy is $\approx 3 \times 10^{-8}$, which is comparable to Geminga (Goldoni et al. 1995). A comparison can be made with the Vela pulsar, which also has a large optical pulsed fraction combined with weakly pulsing thermal X-rays. In contrast to PSR 0656+14, Vela has a high γ-ray flux with a complex optical signature, but the efficiency for producing the optical photons is similar for both pulsars. The sinusoidal shape of the PSR 0656+14 light curve is indicative of a close alignment between the pulsar's rotational axis and the line of sight. Our high pulsed fraction (40%–100%) is significantly higher than the corresponding X-ray pulsed fraction at 9%–30% (Finley, Ögelman, & Kiziloğlu 1992; Possenti, Mereghetti, & Colpi 1996; Greiveldinger et al. 1996). However, it is closer to the observed γ-ray pulsed fraction (Ramanamurthy et al. 1996). Our upper limit to the unpulsed flux is consistent with the predictions of fits to X-ray observations based upon thermal emission enhanced by neutron star atmospheric effects (Pavlov et al. 1996); however, it is important to note that the estimated unpulsed flux is dependent upon the error in the total flux, which is relatively large. From the same analysis, our total and pulsed emission are consistent with a contribution from both the atmospheric thermal emission from hot spots on the surface of the neutron star and nonthermal emission with a power law presumed to come from magnetospheric phenomena (Fig. 4). Future time-resolved observations in low-energy, γ-ray, *R*, and *I* should be compared with UV and EUV studies to separate the contribution from both emission sites.

PSR 0656+14 now becomes the fourth pulsar whose pulses are observed at optical wavelengths. We confirm the previous

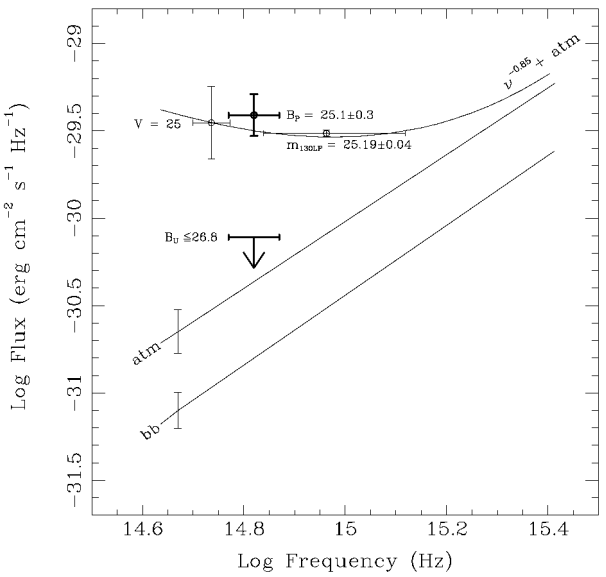

FIG. 4.—The observed optical data compared to extrapolations from the soft X-ray region (Finlay et al. 1992). The *V* data are from Caraveo et al. (1994a), and the UV data are from Pavlov et al. (1996). We show our flux (B_P) and the 1 σ upper limit to the unpulsed flux (B_U).

optical identification (Caraveo et al. 1994a) and show that the pulsed fraction is much higher than in the soft X-ray region. Our observations are in agreement with predictions based upon a composite model of nonthermal magnetospheric and thermal atmospheric emission. From the Pacini and Salvati scaling relationship (Pacini & Salvati 1987) we might expect the nonthermal component to have a *B* magnitude in the range 34–36. Our pulsed magnitude (at 25.1) departs significantly from this and testifies to the nonthermal component of optical radiation of PSR 0656+14 being generated not near the light cylinder (as with the Crab, Vela, and PSR 0540−69 pulsars) but probably nearer the surface of the neutron star. Integrating over this longer path will produce some increase in the luminosity, but such an emission region will be strictly bounded radially by the local magnetic field ($\propto r^{-3}$). However, as the Pacini scaling relationship and its derivatives are restricted to the younger pulsars, where emission can be correctly described as coming from a constant fraction of the light cylinder radius, we would not expect this to scale to these older pulsars. More observations will be necessary with large ($\gtrsim$4 m) telescopes to look for pulsations in all optical bands. These should finally determine what fraction of the emission (both pulsed and unpulsed) is thermal or nonthermal in origin and the spectral index of the pulsed component in the optical bands. This latter measurement is required to understand whether the observed pulsed optical emission is the low-energy tail of the very weak γ-ray emission. Future observations in the crucial low-energy γ-ray, red, and infrared regions as well as the UV (including archival studies of the *EUVE* region) should separate the contribution from a thermal and a magnetospheric source. This would also allow us to determine any differences in the spectral indices in the γ-ray and optical regions.

Modeling of optical emission from middle-aged pulsars is becoming critically important, as observations are showing more discrepancies between predicted emission patterns and those observed. Comparisons between Geminga and PSR 0656+14, both nearby middle-aged pulsars with similar periods and period derivatives, illustrate our current lack of an overall model. In the former we have a middle-aged pulsar with strong γ-ray emission and a possible weak radio emission. In the latter we have maybe a very weak γ-ray emission combined with a relatively strong radio signature. Yet in the optical and soft X-ray region they exhibit a similar behavior. It may well be that viewing geometry plays a critical role in the observed emission for both of these objects.

We are grateful to Patrizia Caraveo and Giovanni Bignami for useful comments and for the provision of their NTT image. We are also grateful to the 6 m telescope Program Committee of the RAS for observing time allocation. We thank the engineers of SAO RAS, A. Maksimov for help in equipment preparation for the observations, V. Komarova for participation in the Letter preparation, and the Director of SAO RAS Yu. Balega for arranging the observations. Fernando Camilo is thanked for the provision of the Jodrell Bank radio timing ephemeris for PSR 0656+14. This work was supported by the Russian Foundation of Fundamental Research, the Russian Ministry of Science and Technical Politics, and the Science Educational Centre "Cosmion." The support of FORBAIRT, the Irish Research and Development agency, is gratefully acknowledged.

REFERENCES

Arzoumanian, Z., Nice, D. J., & Taylor, J. H. 1992, GRO/Radio Timing Database (Princeton: Princeton Univ.)
Arzoumanian, Z., Nice, D. J., & Taylor, J. H., & Thorsett, S. E. 1994, ApJ, 422, 671
Bignami, G. F., & Caraveo, P. A. 1996, ARA&A, 34, 331
Buccheri, R., et al. 1983, A&A, 128, 245
Camilo, F. 1996, private communication
Caraveo, P. A., Bignami, G. F., & Mereghetti, S. 1994a, ApJ, 422, L87
Caraveo, P. A., Mereghetti, S., & Bignami, G. F. 1994b, ApJ, 423, L125
Cocke, W. J., Disney, M. J., & Taylor, D. J. 1969, Nature, 221, 525
Córdova, F. A., Hjellming, R. M., Mason, K. O., & Middleditch, J. 1989, ApJ, 345, 451
Cullum, M. 1990, The MAMA Detector Users' Manual (Garching: ESO)
Finley, J. P., Ögelman, H., & Kiziloğlu, U. 1992, ApJ, 394, L21
Foster, R. S., Edelstein, J., & Bowyer, S. 1996, in IAU Colloq. 152, Astrophysics in the Extreme Ultraviolet, ed. S. Bowyer & R. Malina (Dordrecht: Kluwer), 437
Goldoni, P., Musso, C., Caraveo, P. A., & Bignami, G. F. 1995, A&A, 298, 535
Greiveldinger, C., et al. 1996, ApJ, 465, L35
Halpern, J. P., & Tytler, D. 1988, ApJ, 330, 201
Kurt, V. G., Komberg, B. V., Sokolov, V. V., Zharikov, S. V., & Pavlov, G. G. 1996, IAU Circ. 6533
Landolt, A. U. 1992, AJ, 104, 340
Lyne, A., & Pritchard, R. S. 1996, Crab Timing Ephemeris (Manchester: Univ. Manchester)
Manchester, R. N., et al. 1978, MNRAS, 185, 409
Middleditch, J., & Pennypacker, C. 1985, Nature, 313, 659
Middleditch, J., et al. 1996, Los Alamos Tech. Rep. LAUR 96-3305
Mignani, R., Caraveo, P. A., & Bignami, G. F. 1997, Messenger, 87, 43
Pacini, F., & Salvati, M. 1987, ApJ, 321, 447
Pavlov, G. G., Stringfellow, G. S., & Córdova, F. A. 1996, ApJ, 467, 370
Possenti, A., Mereghetti, S., & Colpi, M. 1996, A&A, 313, 565
Ramanamurthy, P. V., Fichtel, C. E., Kniffen, D. A., Sreekumar, P., & Thompson, D. J. 1996, ApJ, 458, 755
Redfern, R. M., Shearer, A., Wouts, R., O'Kane, P., O'Byrne, C., & Jordan, B. M. 1993, in IAU Colloq. 136, Stellar Photometry: Current Techniques and Future Developments, ed. I. Elliot & C. J. Butler (Cambridge: Cambridge Univ. Press), 137
Shearer, A., Butler, R., Redfern, R. M., Cullum, M., & Danks, A. C. 1996a, ApJ, 473, L115

Shearer, A., Redfern, M., Pedersen, H., Rowold, T., O'Kane, P., Butler, R., O'Byrne, C., & Cullum, M. 1994, ApJ, 423, L51
Shearer, A., et al. 1996b, IAU Circ. 6502
Taylor, J. H., et al. 1993, ApJS, 88, 529
Thompson, R. J., & Córdova, F. A. 1994, ApJ, 421, L13
Thompson, R. J., Córdova, F. A., Hjellming, R. M., & Fomalont, E. B. 1991, ApJ, 366, L83
Timothy, J. G., & Bybee, R. L. 1986, Proc. SPIE, 687, 109
Wallace, P. T., et al. 1977, Nature, 266, 692